MOLECULAR AND CELLULAR BIOLOGY, July 2011, p. 2653–2666 Vol. 31, No. 13
0270-7306/11/$12.00 doi:10.1128/MCB.01358-10

Functional Cooperation between the Proteins Nck and ADAP Is Fundamental for Actin Reorganization▽†

Maor H. Pauker, Barak Reicher, Sophie Fried, Orly Perl, and Mira Barda-Saad*

The Mina and Everard Goodman Faculty of Life Sciences, Bar-Ilan University, Ramat-Gan 52900, Israel

Received 26 November 2010/Returned for modification 7 January 2011/Accepted 11 April 2011

T cell antigen receptor (TCR) activation triggers profound changes in the actin cytoskeleton. In addition to controlling cellular shape and polarity, this process regulates vital T cell responses, such as T cell adhesion, motility, and proliferation. These depend on the recruitment of the signaling proteins Nck and Wiskott-Aldrich syndrome protein (WASp) to the site of TCR activation and on the functional properties of the adapter proteins linker for activation of T cells (LAT) and SH2-domain-containing leukocyte protein of 76 kDa (SLP76). We now demonstrate that Nck is necessary but insufficient for the recruitment of WASp. We show that two pathways lead to SLP76-dependent actin rearrangement. One requires the SLP76 acidic domain, crucial to association with the Nck SH2 domain, and another requires the SLP76 SH2 domain, essential for interaction with the adhesion- and degranulation-promoting adapter protein ADAP. Functional cooperation between Nck and ADAP mediates SLP76-WASp interactions and actin rearrangement. We also reveal the molecular mechanism linking ADAP to actin reorganization.

T cell activation triggers multiple molecular events, including the activation of protein tyrosine kinases (PTKs), formation of multiprotein signaling complexes, and activation of enzymes and transcription factors (25, 37, 47). Cytoskeletal actin reorganization is also dependent on these events initiated at the T cell–antigen-presenting cell (APC) interface, the immunological synapse (IS). Interference with actin dynamics results in an impaired immune response and can induce T cell anergy (40).

We and others (2, 4, 8, 11, 12, 16) have demonstrated complex molecular events linking T cell antigen receptor (TCR) activation to actin rearrangement. One major pathway, mediated by the activation of multiple PTKs, leads to phosphorylation of the adapter molecules linker for activation of T cells (LAT) and SH2-domain-containing leukocyte protein of 76 kDa (SLP76). Phosphorylation of SLP76 leads to recruitment of the Nck adapter molecule, which is associated with key regulators of the actin cytoskeleton Wiskott-Aldrich syndrome protein (WASp) and WAVE2.

The molecular structure of SLP76 consists of an N-terminal sterile-alpha motif (SAM) (41), an acidic domain containing tyrosine residues subject to phosphorylation, a central proline-rich region, and a C-terminal SH2 domain. Phosphorylation of the tyrosines allows the interaction of SLP76 with the adapter Nck, the Rho-family GEF, VAV, and Itk, all via their SH2 domains (5, 8, 48, 49, 51). The interactions of SLP76, Nck, and VAV are essential for the activation of WASp and its recruitment to the IS (51). TCR engagement also induces the association of the SLP76 SH2 domain with the adhesion- and degranulation-promoting adapter protein (ADAP) and to the serine-threonine kinase hematopoietic progenitor kinase 1 (HPK-1) (38). In addition to SLP76, ADAP is capable of binding other proteins, and it is recruited to the IS (26, 35). The role of ADAP in integrin function has been explored (10, 23, 36, 46); however, its involvement in actin cytoskeleton reorganization is controversial (18, 22, 35, 43). Currently, the molecular mechanism by which ADAP regulates the actin machinery remains unclear.

WASp has been implicated in a variety of cellular processes associated with dynamic actin-mediated events, such as membrane structure formation (e.g., lamelliopodia or filopodia), vesicular trafficking, and endocytosis (3). The role of WASp in actin filament formation depends on two distinct processes, WASp recruitment to the T cell-APC contact site and its functional activation, triggered by the Rho GTPase, Cdc42, and phosphorylation on Y291 (1, 44). In addition to WASp, WAVE2 was shown to control actin reorganization and integrin-dependent adhesion in T lymphocytes (33, 52) Notwithstanding the extensive characterization of multiple signaling proteins regulating actin polymerization, their mechanisms of interaction and the potential for molecular cooperation between them have not been fully explored. Here, we demonstrate a functional cooperation between Nck and ADAP in stabilizing the recruitment of WASp to SLP76 and thus in regulating actin rearrangement.

MATERIALS AND METHODS

Reagents. Mouse anti-CD3ε (UCHT or HIT3a) and anti-CD28 were purchased from BD Pharmingen. The expression vectors pEYFP-N1, pEYFP-C1, and pECFP-C1 were obtained from Clontech, and pcDNA3.1$^+$/Hygro was obtained from Invitrogen. Antibodies or reagents were obtained from the following suppliers: anti-WASp and anti-Nck from Santa Cruz Biotechnology and Upstate Biotechnology, respectively; anti-SLP76 from Antibody Solutions; anti-green fluorescent protein (GFP) from Roche; anti-ADAP from BD Transduction Laboratories; and phalloidin from Molecular Probes. Alexa Fluor-conjugated, isotype-specific secondary antibodies were purchased from Molecular Probes.

Pools of the following three independent specific RNA duplexes for human SKAP1 were purchased from Invitrogen: UGGCAGAAGGUUUGCGGAAU

* Corresponding author. Mailing address: Faculty of Life Sciences, Bar-Ilan University, Ramat-Gan 52900, Israel. Phone: 972-3-5317311. Fax: 972-3-7384058. E-mail: bardasm@mail.biu.ac.il.

† Supplemental material for this article may be found at http://mcb.asm.org/.

▽ Published ahead of print on 2 May 2011.

GAGAA, UUCUCAUUCCGCAAACCUUCUGCCA, and GGAGCUCAAG AACUUGAUAACGUAA.

Pools of the following independent specific RNA duplexes were purchased from Dharmacon: human Fyb small interfering RNA (siRNA) oligonucleotides GAGAUGAAGUUUACGAUGA, GAAGAUAGAUGCUGCUAAG, GCAA AGGCCAGACGUCUUA, and AACCAGAGAUCUACAGGUA; human Nck1 siRNA oligonucleotides ACUAAAAGCACAAGGGAAA, AGAAAUG GCAUUAAAUGAA, and GAUAGUGAAUCUUCGCCAA; and human Nck2 siRNA oligonucleotide CUUAAAGCGUCAGGGAAGA.

Plasmid construction and GFP mutations. Human Nck cDNA and human WASp cDNA were kindly provided by B. Mayer from the Connecticut University Health Center, Farmington, CT, and by D. Nelson from the National Cancer Institute, National Institutes of Health, Bethesda, MD, respectively. The cDNAs were cloned into expression vector pECFP-C/N or pEYFP-C/N to obtain cyan fluorescent protein (CFP) or yellow fluorescent protein (YFP)-tagged proteins. *Aequorea* GFP derivatives were rendered monomeric by the A206K substitution described by D. A. Zacharias et al. (50).

Primary cell culture, cell transfection, and generation of stable cells. Human T lymphocytes were prepared from the peripheral blood of healthy donors as described previously (27). Cells were transfected with an Amaxa electroporator using Amaxa solution. Transiently transfected T cell cultures and stable clones were used in this study. Stable clones were derived from transiently transfected cells using a combination of drug selection and cell sorting. Cell fluorescence analysis and cell sorting were performed on a FACSVantage (BD Biosciences).

Cellular and live-cell imaging. Dynamic fluorescent and interference reflection microscopy (IRM) images were collected on a Zeiss 510 Meta confocal microscope. Image stacks were collected over time, using an autofocusing algorithm based on reflection images obtained by imaging the plane of the T cell-cover glass contact. All images were collected using a 63× Plan-Apochromat objective (Carl Zeiss). For live-cell imaging, a hot-air blower (Nevetec) was used to maintain the sample at 37°C. Fine adjustments were made by using a digital temperature probe to monitor the buffer temperature in the chamber. Image processing and measurements were performed using IPLab software, version 3.9.

Spreading assay. Chambered cover glasses (LabTek) were cleaned by treatment with 1 M HCl, 70% ethanol for 30 min and dried at 60°C for 30 min. The chambers were treated with a 0.01% (wt/vol) poly-L-lysine solution (Sigma) for 5 min, drained, and dried at 60°C for 30 min. Chambers were coated with stimulatory monoclonal antibodies (10 μg/ml) overnight at 4°C, using anti-CD3 for Jurkat cells or anti-CD3 and anti-CD28 for primary cells. Excess antibody was removed by extensive washing with phosphate-buffered saline (PBS). Cells were seeded onto chambers containing imaging buffer (RPMI medium without phenol red containing 10% fetal calf serum [FCS] and 25 mM HEPES). T cells were seeded over the bottom of chambers in 100 μl of imaging buffer at a concentration of 2×10^6 cells/ml for the times indicated below. Cells were fixed for 25 min with 4% paraformaldehyde in PBS followed by permeabilization with 0.1% Triton X-100 for 5 min. Cells were blocked for 1 h in PFN buffer (PBS without Ca^{+2} and Mg^{+2} and containing 10% FCS and 0.02% azide) containing 2% normal goat serum (Jackson ImmunoResearch). Cells were incubated with the indicated primary antibodies and diluted in blocking medium for 1 h, followed by staining with isotype-specific Alexa Fluor-conjugated antisera for 30 min. Cells were washed three times with PFN between steps.

FRET analysis. Fluorescence resonance energy transfer (FRET) was measured by the donor-sensitized acceptor fluorescence technique. Three sets of filters were used: one optimized for donor fluorescence (excitation, 468 nm, and emission, 475 to 505 nm), a second for acceptor fluorescence (excitation, 514 nm, and emission, 530 nm longpass [LP]), and a third for FRET (excitation, 468 nm; emission, 530 nm LP). FRET was corrected as described below, and the FRET efficiency was determined.

FRET correction. The non-FRET components were calculated and removed using calibration curves derived from images of single-labeled CFP- or YFP-expressing cells. Sets of reference images were obtained using the same acquisition parameters as were used for the FRET experimental images. To correct for CFP "bleed through," the intensity of each pixel in the CFP image from CFP-expressing cells was compared to the equivalent pixel in the FRET image of the same cells. A calibration curve was derived that defined the amount of CFP fluorescence seen in the FRET image as a function of the fluorescence in the CFP image. A similar calibration curve was obtained defining the amount of YFP fluorescence appearing in the FRET image as a function of the intensity in the YFP image, using images of cells expressing only YFP. Separate calibration curves were derived for each set of acquisition parameters used in the FRET experiments. Then, using the appropriate calibration curves, together with the CFP and YFP images, the amount of CFP bleed through and YFP cross-excitation was calculated for each pixel in the experimental FRET images. These non-FRET components were subtracted from the raw FRET images, yielding corrected FRET images.

FRET efficiency calculation. The FRET efficiency ($FRET_{eff}$) was calculated on a pixel-by-pixel basis with the following equation: $FRET_{eff} = FRET_{corr}/(FRET_{corr} + CFP) \times 100\%$, where $FRET_{corr}$ is the pixel intensity in the corrected FRET image and CFP is the intensity of the corresponding pixel in the CFP channel image.

To increase the reliability of the calculations and to prevent low-level noise from distorting the calculated ratio, we excluded pixels below 50 intensity units and saturated pixels from the calculations and set their intensities to zero. These pixels are shown in black in the "pseudocolored" FRET efficiency images.

To estimate the importance of the FRET efficiency values obtained and to exclude the possibility of obtaining false-positive FRET results, we prepared cells expressing free CFP and free YFP as negative controls. The FRET efficiency in the negative-control system was measured and calculated in the same way as in the main experiment. FRET efficiency values obtained from the negative-control samples were subtracted from the values obtained in the main experiments.

Image processing and quantitation. The acquired images were extracted with the LSM browser (Carl Zeiss) and cropped and composed into figures within Adobe Photoshop.

Colocalization analysis. Colocalization was detected by two different methods as previously described (14, 30, 42). For the colocalization analysis based on fluorescence intensity peak, positive colocalization was defined by two simultaneous criteria: (i) the signal from one channel accumulated at the same site of the other channel to more than 2-fold above the basal signal and (ii) at least half of one fluorophore intensity peak overlapped with at least half of the other fluorophore intensity peak. All quantitations were performed on unprocessed 8-bit grayscale images with no saturated pixels. The mean intensity of fluorescence and the line profiles were determined using ImageJ. Statistical analysis was performed using a standard Student's *t* test (14, 30).

In addition, colocalization analysis was performed by determining the Pearson's colocalization correlation coefficient, generated as previously described (42), for each colocalization experiment. Imaris 4.2 software (Bitplane AG, Zurich Switzerland) was used to distinguish between actual colocalization and random association between signals from two labels in the entire three-dimensional image. Pearson's colocalization coefficient varies from −1 to 1, when 1 means perfect colocalization and −1 means perfect exclusion.

Actin shape index. A quantitative estimate of the actin shape changes was obtained as previously described (17), with some modifications, using the following equation: actin shape index $= P^2/4\pi S$, where P and S are the perimeter and the surface of the cell, respectively. These values were obtained by thresholding images of phalloidin staining to outline the polymerized actin. A perfectly circular shape of the polymerized actin yields a shape index of 1, and departure from a circle yields a shape index larger than 1. Colocalization was measured following 1 to 3 min of stimulation, when cluster formation is optimal. However, actin reorganization was determined following 5 min of activation, which is the best time for observing this process.

Immunoblotting and immunoprecipitation. Cells were either stimulated with anti-TCR C305 for 2 min or left untreated. The optimal concentration of the stimulatory antibody was determined by titration. Protein A/G plus-Agarose beads (Santa Cruz Biotechnology) were used for immunoprecipitation. Protein samples were resolved with sodium dodecyl sulfate-polyacrylamide gel electrophoresis (SDS-PAGE), transferred to nitrocellulose membrane, and immunoblotted with appropriate primary antibodies. Immunoreactive proteins were detected with either anti-mouse or anti-rabbit horseradish peroxidase-coupled secondary antibody followed by detection with enhanced chemiluminescence (Pierce) (7).

Statistical analyses. Standard errors were calculated with the use of Microsoft Excel. Statistical significances were calculated in Excel, with Student's *t* tests used for unpaired, two-tailed samples. In all cases, the threshold *P* value required for significance was 0.05.

RESULTS

Recruitment of WASp TCR-induced clusters is dependent on SLP76. We have previously shown that WASp is recruited to the TCR immediately upon activation (4). WASp colocalizes with SLP76, Nck, and other multiple signaling molecules in small clusters. To determine the role of SLP76 in WASp recruitment, we stably expressed WASp fused to CFP in SLP76-deficient J14 T cells. SLP76 deficiency abolished WASp recruitment to the TCR-induced clusters. Reconstitution of

these cells with wild-type (wt) SLP76 restored WASp recruitment (see Fig. S1A in the supplemental material). High FRET (27.8% ± 8.7% [mean ± standard error]) was detected between SLP76-YFP and WASp-CFP (see Fig. S1B in the supplemental material), indicating a close and stable interaction between these molecules.

Actin rearrangement and the association between SLP76 and WASp do not depend solely on the functional activity of Nck. Nck has been shown to mediate the interaction of SLP76 and WASp (8). To assess the requirement of Nck for actin rearrangement, E6.1 Jurkat T cells expressing actin-GFP were treated with siRNA specific for the Nckα,β isoforms, which resulted in a >90% reduction of Nck expression (see Fig. S2A in the supplemental material). Imaging analysis indicated that silencing either Nckα or β had no discernible effect on actin filament formation (Fig. 1A). Inhibition of both Nckα and β simultaneously caused an impairment in actin rearrangement and lamellipodium formation, as detected by measurements of the actin shape index. The actin shape index provides a mathematical representation of the cell's contour, i.e., perimeter and area, and reflects the cell's spreading. A perfectly spread cell with normal morphology yields a circular shape of the polymerized actin, i.e., an index of 1; an impaired actin cytoskeletal rearrangement results in departure from a circle and yields a shape index larger than 1. In the experiment whose results are shown in Fig. 1A, cells treated with siRNA specific to Nckα or β exhibited an actin shape index similar to that of control cells treated with nonspecific (NS) siRNA and close to 1. However, cells gene silenced for Nckα and β presented a significantly higher actin index of ~2.5 ($P \leq 0.0002$). These results show that Nckα and Nckβ share a redundant role in actin cytoskeletal reorganization and that the elimination of both Nck isoforms partially impairs this process.

Previously, we showed a stable interaction between SLP76 and WASp following TCR engagement (4, 6). In the current study, we tested whether Nck is required for this association. J14 cells reconstituted with SLP76-YFP and stably expressing WASp-CFP were treated with siRNA specific to Nckα,β. A slight decrease in their Pearson's colocalization coefficient was detected ($P \leq 0.67$) (Fig. 1B). These results suggest that the model in which only Nck mediates the interaction between SLP76 and WASp is incomplete and that other molecules are involved.

It was previously shown that the SLP76 acidic domain is required for recruitment of the Nck-WASp complex, via the Nck SH2 domain, to the TCR complex (51). As another way of analyzing the Nck-SLP76 interaction, we reassessed the role of the Nck SH2 domain in the recruitment of Nck to SLP76. We stably expressed CFP-Nck conjugates bearing an SH2 domain deletion (CFP-NckΔSH2) in J14 cells reconstituted with SLP76-YFP. The SH2 domain deletion insignificantly reduced TCR-induced clustering of Nck but did not abrogate it ($P \leq 0.94$) (Fig. 1C; also see Video S1 in the supplemental material). The Pearson's colocalization coefficient was used to measure colocalization between SLP76 and Nck wt versus its colocalization with ΔSH2 Nck. This colocalization was evident in the clusters, as indicated by the overlay images (Fig. 1C, yellow).

The SH2 domain of Nck does not exclusively mediate the binding to SLP76. Nck dimerization has been reported to be very weak and unlikely to be physiologically relevant (31). However, to rule out the possibility that the mutant, tagged Nck forms are recruited to the TCR complex by endogenous Nck, we performed several experiments. Nck gene-silencing experiments were done with the aim to target only the endogenous molecules by using siRNA oligonucleotides corresponding to the Nck SH2 domain (see Fig. S2B to D in the supplemental material). J14 cells expressing SLP76-YFP CFP-NckΔSH2 and transfected with the Nck SH2 domain-specific siRNA achieved about 90% downregulation of endogenous Nck (47 kDa) without affecting the truncated CFP-NckΔSH2 molecule (~59 kDa) (see Fig. S2C in the supplemental material). Knockdown of full-length Nck did not abolish CFP-NckΔSH2 clusters (see Fig. S2D and Video S1 in the supplemental material), suggesting that either WASp interacts directly with SLP76 in the absence of Nck or that other signaling proteins stabilize the SLP76-WASp interaction and recruit Nck in a manner independent of the SH2 domain.

Next, we focused on actin rearrangement and investigated whether the expression of SLP76 Y3F (mutated in tyrosines 113, 128, and 145, known as Nck binding sites) (5) has an effect similar to that of gene-silenced Nck on the actin shape index. Actin rearrangement was compared in J14 cells gene silenced for Nck and expressing SLP76 wt versus J14 cells expressing SLP76 Y3F. Our data clearly indicate no significant difference in the actin shape index between these two experimental groups ($P \leq 0.38$) (see Fig. S2E in the supplemental material).

The results of these experiments (Fig. 1C; also see Fig. S2 in the supplemental material) are consistent with the notion that the SH2 domain of Nck does not exclusively mediate the binding to SLP76 and suggest an alternative pathway for Nck recruitment to the SLP76-nucleated complex.

SLP76 SH2 domain is required for interaction with WASp following TCR stimulation. The phosphorylation of WASp at Y291 is critical for the release of WASp autoinhibitory structural constraints and induction of its effector functions, including NFAT activity, actin polymerization, and immunological synapse formation (3, 13). Phosphorylation at a WASp tyrosine residue raises the possibility that WASp activation can induce an interaction at this site with SH2 domain-containing signaling effectors, such as SLP76. Thus, J14 cells expressing SLP76 with an SH2 mutant tagged with YFP (R448K, SLP76*SH2-YFP) were derived and the interaction between SLP76 and WASp was detected and compared to that of J14 reconstituted with SLP76 wt (see Fig. S3A in the supplemental material). Coprecipitation of WASp and SLP76 was observed in the presence of SLP76 wt and, to a lesser extent, in the presence of the SLP76 with the mutated SH2, implying an alternative pathway of WASp recruitment to the SLP76 signaling complex.

Since biophysical data eliminate the possibility that WASp phosphotyrosines bind directly to the SLP76 SH2 domain (data not shown), we checked whether an SLP76 SH2-associated protein, i.e., ADAP, mediates this interaction. Previously, it was suggested that phosphorylation of ADAP enables its association via tyrosine 651 to the SLP76 SH2 domain (15, 19, 32). In order to check this interaction *in vivo*, we incorporated a point mutation, Y651F, in ADAP and determined the binding between ADAP and SLP76 using molecular imaging. As seen in Fig. S3B in the supplemental material, the FRET efficiency between SLP76 and ADAP Y651F versus that be-

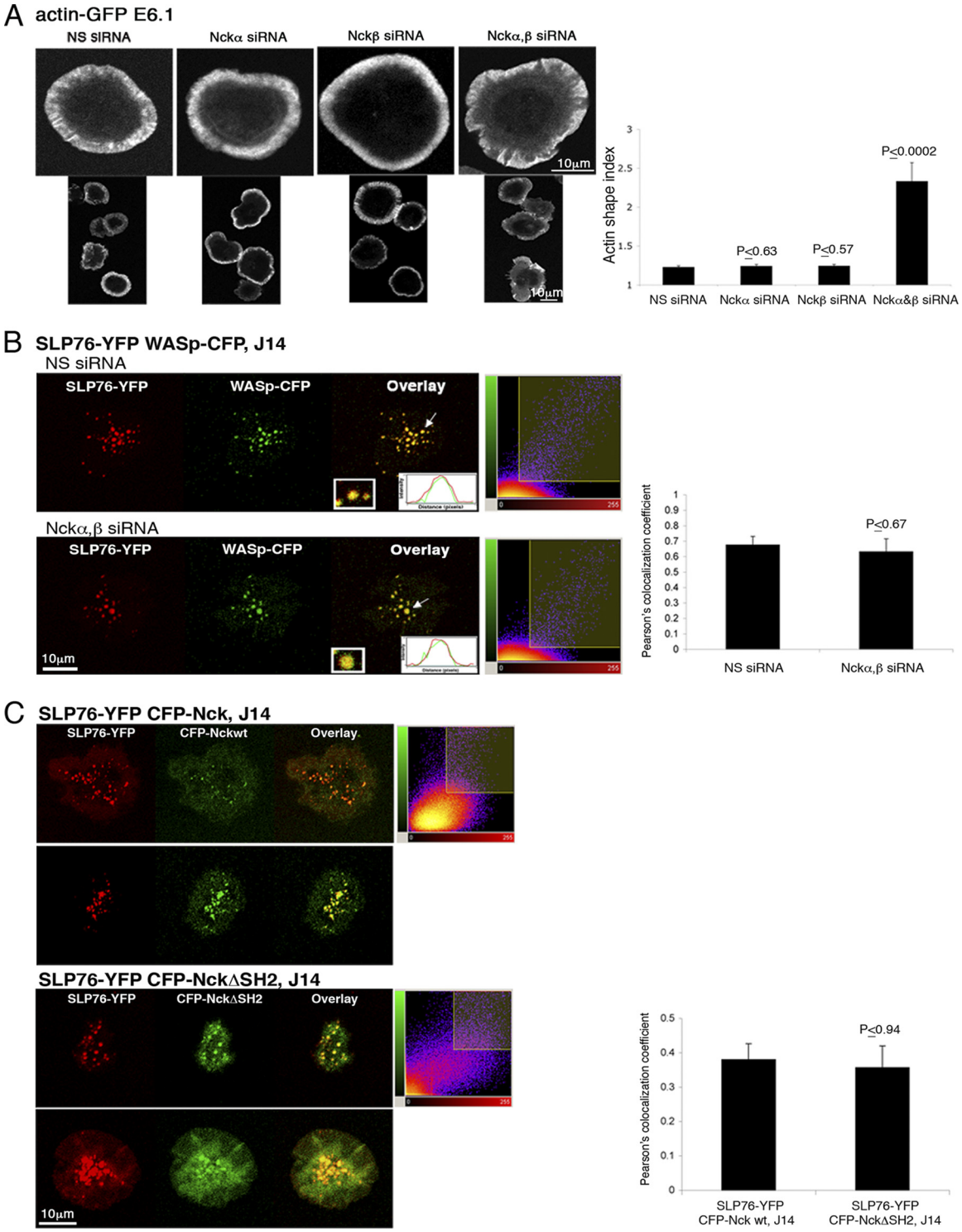

FIG. 1. Actin polymerization and the recruitment of WASp to SLP76 signaling clusters are not solely dependent on Nck. (A) Cells were plated, fixed, and stained with phalloidin. Confocal images were collected after 5 min of activation. In the right panel, the results of >4 independent experiments are presented The actin shape index was determined as described in Materials and Methods. *t* tests were performed to compare the results of nonspecific (NS) siRNA treatment with the results for other experimental groups; error bars show standard errors. (B) SLP76-deficient J14 cells expressing SLP76-YFP and WASp-CFP were treated with siRNA specific to Nckα,β. Cells treated with NS siRNA served as a negative control. After 48 h, cells were plated and activated for 3 min as described for panel A. Overlays (insets) of the fluorescence peaks of the punctae are shown. Colocalization analysis is based on these fluorescence intensity peaks and was further analyzed by obtaining Pearson's colocalization coefficients (scatter diagrams). Imaging analysis was performed on more than 50 cells for each experimental group. (C) The association of Nck with SLP76 is not exclusively dependent on the Nck SH2 domain. J14 T cells expressing SLP76-YFP and the indicated CFP-Nck forms (wt or SH2 domain deletion [NckΔSH2]) were seeded on stimulatory coverslips. Live-cell images were collected 3 min after activation. Two out of 30 cells are presented for each experimental group. The combined images (overlays) are presented. A *t* test was performed, comparing the colocalization of CFP-Nck wt clusters with SLP76-YFP to the colocalization of the CFP-NckΔSH2 mutant with SLP76-YFP.

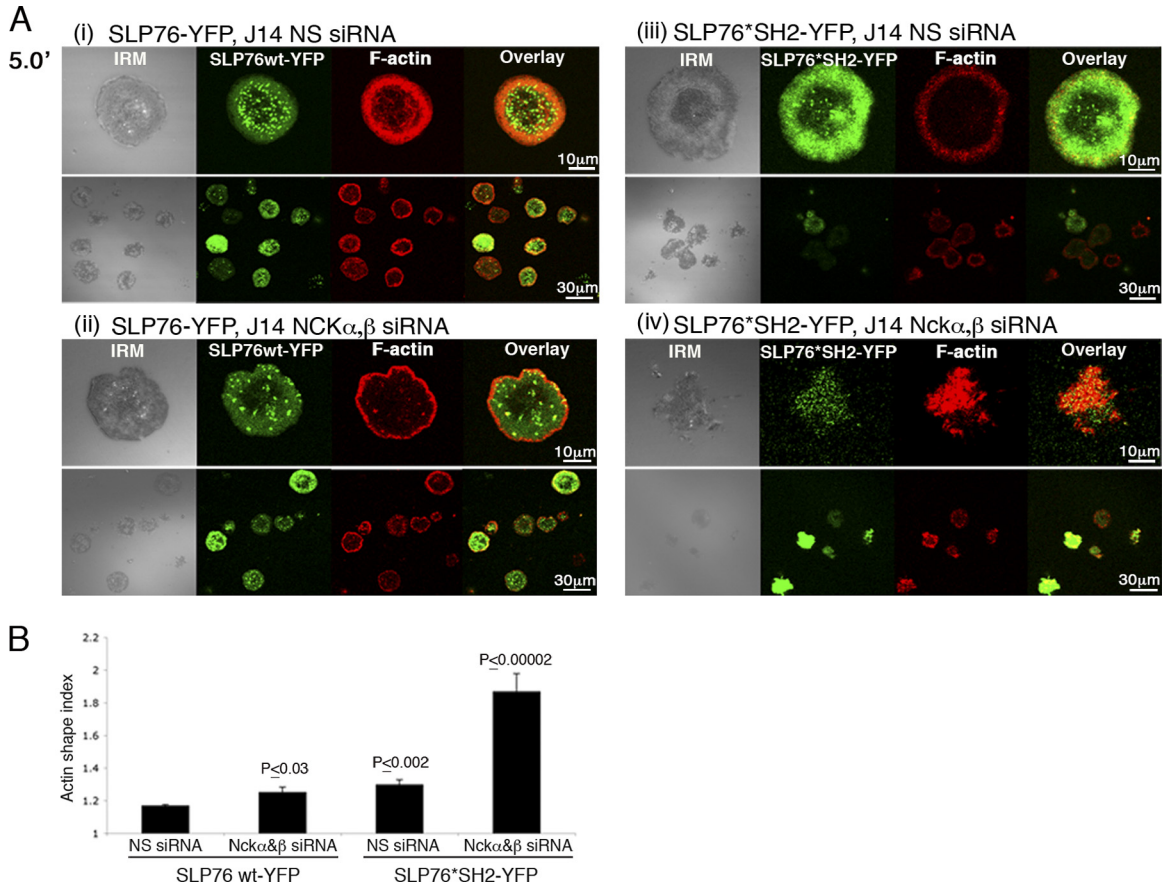

FIG. 2. The SH2 domain of SLP76 is important for stabilization of SLP76 signaling clusters and for actin polymerization. (A) J14 cells expressing the SLP76 SH2 mutant form (R448K, *SH2) or SLP76 wt tagged with YFP were treated with siRNA specific to Nckα,β or NS siRNA. After 48 h, cells were plated, fixed, and stained with phalloidin 5 min (5.0′) into the spreading process (Ai to iv). IRM and combined fluorescence images (overlay) are presented. (B) The results of three independent experiments are summarized. Significant differences were found in actin rearrangement as determined by the actin shape index of SLP76 wt-YFP cells treated with NS siRNA compared to the results for the other experimental groups. A *t* test analysis between SLP76 wt-YFP and SLP76*SH2-YFP, treated with Nck siRNA, was performed, and the *P* value was found to be ≤0.00002. Error bars show standard errors.

tween SLP76 and ADAP wt was dramatically reduced, to 9.1 ± 2 versus 16.9 ± 0.6, respectively ($P \leq 0.002$). Our results, obtained by an *in vivo* system, support the evidence suggesting that the phosphorylated ADAP Y651 residue interacts directly with the SLP76 SH2 domain and partially mediates the interaction between SLP76 and ADAP (15, 19, 32, 46).

The SH2 domain of SLP76 is critical for stabilization of SLP76-containing signaling clusters and for actin rearrangement. SLP76 interactions with WASp, independent of Nck, might be mediated by the SLP76 SH2 domain. To assess the potential role of this domain in the cytoskeletal reorganization induced by TCR activation, J14 cells expressing SLP76*SH2-YFP were used. The dynamic behavior of SLP76*SH2-YFP during the stimulation of J14 cells was dramatically different from that of SLP76 wt-YFP (see Videos S2A and B in the supplemental material). While the latter was recruited into mobile clusters that moved from the cell periphery to the center along microtubules, as previously reported (4, 9), the mutant chimeras were assembled into short-lived clusters and moved randomly.

When actin was examined, the SH2 mutation appeared to have a slight effect on actin rearrangement in J14 cells reconstituted with SLP76*SH2-YFP compared to the results obtained with SLP76 wt-YFP (as determined by the actin shape index; $P \leq 0.002$) (Fig. 2Ai versus Aiii and B). However, the additional application of Nckα,β siRNA to the SLP76*SH2-YFP-reconstituted cells resulted in the severe impairment of actin cytoskeletal rearrangement (Fig. 2Ai versus Aiv and B; $P \leq 0.00002$) in comparison to that in the corresponding SLP76 wt-YFP cells, indicating the importance of Nck in this system. Furthermore, these results suggest that the SLP76 SH2 domain mediates an alternative route of actin regulation, possibly by the indirect binding of the SLP76 SH2 domain to WASp. The SLP76 SH2 domain can partially compensate for disruption of the Nck-dependent pathway.

ADAP is recruited to the activated TCR site, colocalizes with ZAP-70 and SLP76, and migrates with WASp to sites of actin rearrangement. In view of the association of ADAP, when phosphorylated at Y651, with the SH2 domain of SLP76, we asked whether ADAP could contribute to TCR-mediated actin polymerization. Immunostaining experiments revealed colocalization of ADAP with SLP76 and pZAP-70 in signaling

clusters. A significant portion of ADAP molecules was also found at the perimeter of the cell, where the actin ring is located, particularly after 5 min of activation (see Fig. S4 in the supplemental material).

To assess the dynamic behavior of ADAP following TCR stimulation, J14 cells reconstituted with either SLP76-YFP or SLP76*SH2-YFP were stably transfected with ADAP tagged with CFP. Molecular imaging demonstrated that ADAP-CFP was rapidly recruited to signaling clusters with SLP76-YFP. However, after 5 min of activation, some ADAP translocated to the perimeter of the cells and was diffused (Fig. 3A). FRET analysis between ADAP and SLP76 was performed. An average FRET efficiency of about 16.9% ± 0.9% was observed, mainly at the signaling clusters and less at the periphery (Fig. 3A, top). When the SLP76 SH2 domain was mutated, a few short-lived clusters of SLP76 were observed (within 1 min of activation) along with a dispersed pattern of ADAP, not necessarily correlated with the clusters. A dispersed FRET signal of about 10.5% ± 1.45% was measured between ADAP and SLP76*SH2 ($P \leq 0.0002$) (Fig. 3A, bottom). Although a significant reduction of FRET efficiency was measured in cells expressing SLP76*SH2 compared to the FRET efficiency in those expressing SLP76 wt, a constitutive interaction between ADAP and SLP76*SH2 was detected (Fig. 3A and B). Since recent studies using the two-hybrid system suggested that ADAP associates directly with Nck (28), we checked whether SLP76-ADAP interaction is also supported by Nck. J14 cells reconstituted with SLP76*SH2-YFP and stably expressing ADAP-CFP were gene silenced to Nckα,β, and the FRET efficiency between ADAP and SLP76*SH2-YFP was determined. Our data clearly indicate a dramatic reduction in their interaction (2.4 ± 1.6; $P < 0.00004$) (Fig. 3B).

To understand the role of ADAP in the dynamic localization of SLP76, we used J14 cells expressing SLP76-YFP and transiently transfected with either siRNA directed at ADAP or an NS siRNA. The NS siRNA had no deleterious effects on SLP76 cluster formation or trafficking. Live-cell imaging of activated T cells, in the setting of decreased ADAP expression, revealed the formation of randomly moving, short-lived SLP76 clusters, similar to the pattern observed in SLP76*SH2-YFP J14 cells (see Videos S3A and B in the supplemental material). To further follow the dynamic localization of ADAP and determine its relationship to WASp and its dependency on SLP76, ADAP-YFP and WASp-CFP were simultaneously expressed in either E6.1 (Fig. 4A, top) or SLP76-deficient J14 cells (Fig. 4A, bottom). In the presence of SLP76, colocalization between ADAP and WASp was observed from the moment of stimulation and throughout the spreading process (Fig. 4A, top, and Fig. 4B). However, the distribution of the ADAP-WASp complex was extremely altered in the absence of SLP76. No recruitment to the TCR site was observed; instead, the complex remained homogenously dispersed in the cytosol. Interestingly, no significant difference was obtained in FRET efficiency between WASp and ADAP in the presence (19.5% ± 1.95%) or absence of SLP76 (16.02% ± 0.7%; $P \leq 0.06$) (Fig. 4A and B). The expression levels of the fluorescence proteins used for FRET analysis in this study were determined by Western blot analysis (see Fig. S5A in the supplemental material).

To corroborate the interactions observed using imaging techniques, we evaluated the interaction of WASp or SLP76-YFP with ADAP by immunoprecipitating WASp or SLP76-YFP and blotting with anti-ADAP sera. The results confirmed the FRET analysis and indicated a constitutive association between WASp and ADAP in the presence of SLP76 wt (J14/SLP76 wt) or mutated SLP76 (J14/SLP76*SH2) (see Fig. S5B, top left, in the supplemental material). Furthermore, coprecipitation of WASp and ADAP was observed in the presence (J14/SLP76-YFP) and in the absence of SLP76 (J14) (see Fig. S5B, top right, in the supplemental material).

The interaction between SLP76 and ADAP was detectable in unstimulated and stimulated cells. An interaction between SLP76 and ADAP also occurred in J14 cells expressing SLP76*SH2-YFP (see Fig. S5B, bottom, in the supplemental material), suggesting some independence of this interaction on a functional SLP76 SH2 domain.

Both Nck and ADAP participate in stabilizing the SLP76 interaction with WASp. The results described thus far indicate that (i) the SLP76-WASp interaction is not solely dependent on Nck, (ii) ADAP-WASp colocalization is independent of SLP76, (iii) the SLP76 SH2 domain contributes to signaling complex formation and actin polymerization, and (iv) the SLP76-ADAP interaction does not necessarily depend on the SLP76 SH2 domain. We next decided to assess the relative contributions of Nck and ADAP to the process of WASp recruitment using gene-silencing experiments. J14 cells expressing SLP76-YFP and WASp-CFP were transiently transfected with siRNA specific for Nckα,β or ADAP (see Fig. S6A in the supplemental material). Cells transfected with NS siRNA served as a control. As shown before, a high-resolution colocalization and a high FRET efficiency (Fig. 5A; also see Fig. S1B in the supplemental material), about 27.8% ± 8.7%, were measured between SLP76 and WASp. Cells transfected with siRNA to Nckα,β or ADAP exhibited lower FRET efficiencies, about 10.8% ± 4.9% ($P \leq 0.06$) and 9.5% ± 4.65 ($P \leq 0.01$), respectively (Fig. 5A). Silencing of ADAP and Nckα,β together dramatically reduced colocalization and abolished the occurrence of FRET measured between SLP76 and WASp ($P \leq 0.001$) (Fig. 5A). Interestingly, the FRET efficiency values for the SLP76*SH2-YFP interaction with WASp-CFP were similar to those obtained with SLP76-YFP and WASp-CFP in cells treated with ADAP siRNA (Fig. 5A). A significant reduction ($P \leq 0.01$) was found in the Pearson's colocalization coefficient or FRET efficiency between WASp-CFP and SLP76*SH2-YFP versus that between WASp-CFP and SLP76 wt-YFP, suggesting that ADAP plays a role in stabilizing the interaction between SLP76 and WASp via its interaction with the SLP76 SH2 domain (Fig. 5A; see Fig. S6B in the supplemental material).

Loss of ADAP was previously shown to induce degradation of SKAP1 (24). In order to check whether the effects observed with ADAP suppression might have occurred due to the suppression of SKAP1, SLP76-YFP- and WASp-CFP-expressing cells were treated with siRNA specific to SKAP1, and the interaction between SLP76 and WASp was determined by FRET analysis. Our data demonstrated no effect of SKAP1 downregulation ($P \leq 0.74$) on this interaction (see Fig. S6C in the supplemental material).

The FRET between SLP76 and ADAP was measured in the presence or absence of a point mutation that inactivates the

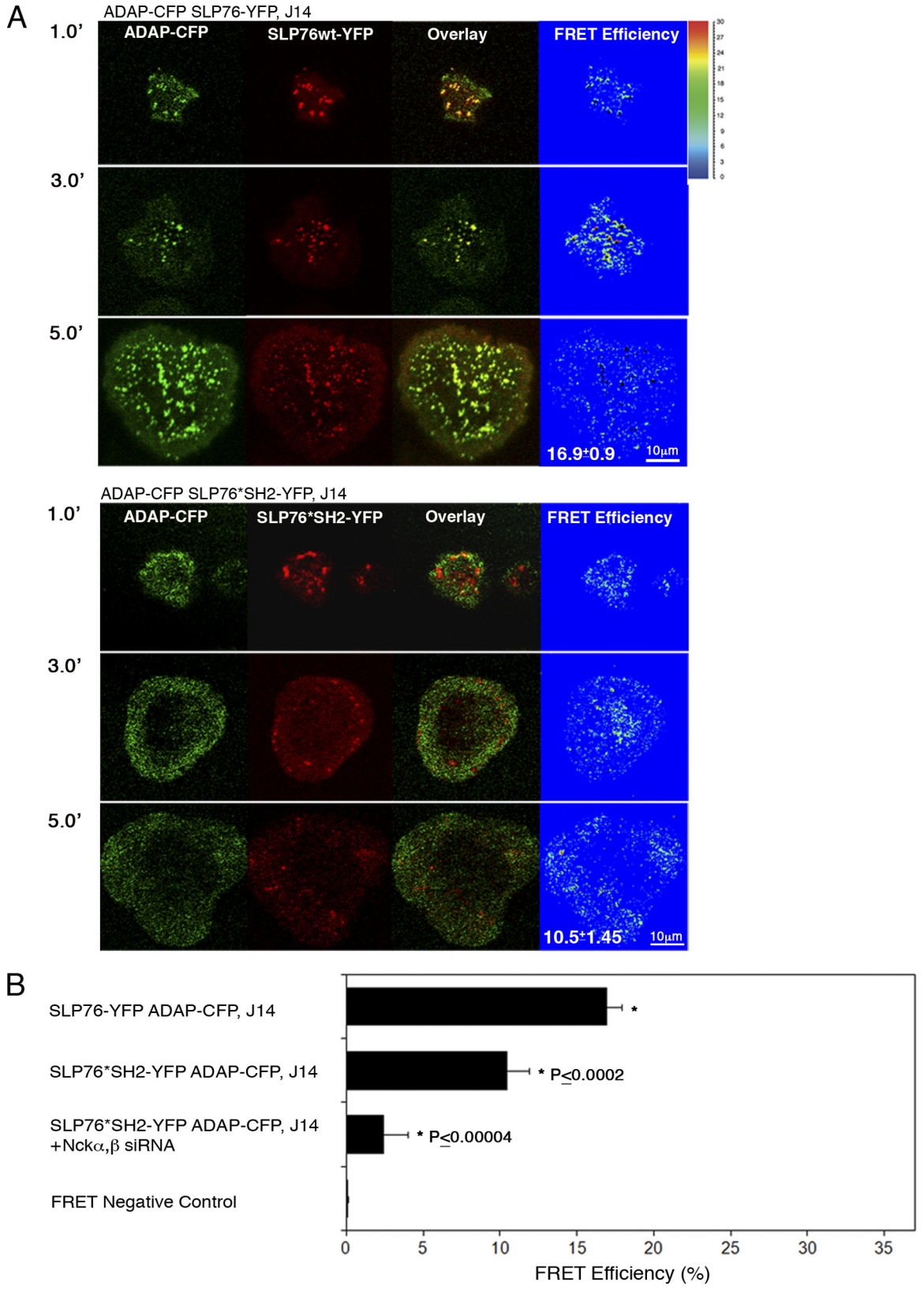

FIG. 3. ADAP recruitment to TCR-induced clusters is dependent on SLP76. (A) SLP76-deficient cells stably reconstituted with SLP76 wt or SLP76*SH2 tagged with YFP were transfected with ADAP-CFP. FRET analysis between SLP76-YFP and ADAP-CFP is presented. A slight but significant reduction in FRET efficiency between ADAP and SLP76*SH2 was measured in comparison to that between ADAP and SLP76 wt ($P \leq 0.0002$). 1.0′, 3.0′, and 5.0′ indicate minutes of activation. (B) FRET analysis of the molecular associations between ADAP and SLP76 wt versus those between ADAP and SH2 mutant SLP76 is shown. J14 cells expressing SH2 mutant SLP76-YFP and ADAP-CFP were pretreated with specific Nck siRNAs. Cells were seeded and fixed 3 min after the initiation of spreading. The average value of FRET efficiency ± standard error obtained for each given pair is presented. The data shown are representative of >3 independent experiments.

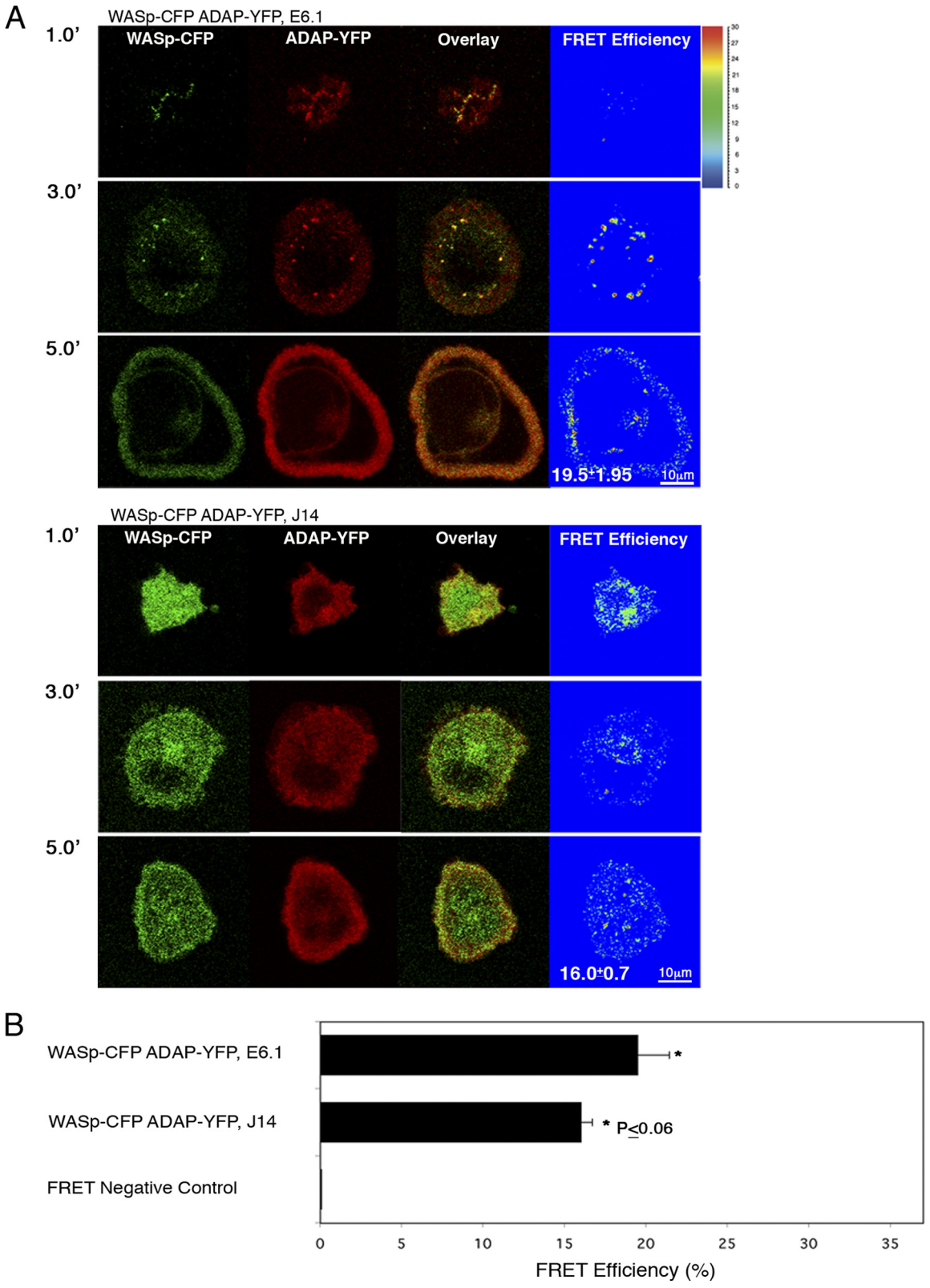

FIG. 4. The association between ADAP and WASp is independent of SLP76. E6.1 Jurkat T cells or SLP76-deficient J14 cells stably reconstituted with WASp-CFP were transfected with ADAP-YFP. Cells were plated, and FRET efficiency between ADAP and WASp was determined. No significant difference was measured between the two molecules in the presence versus the absence of SLP76 ($P \leq 0.06$). 1.0′, 3.0′, and 5.0′ indicate minutes of activation. (B) FRET analysis of the molecular associations between WASp and ADAP. J14 or E6.1 cells expressing WASp-CFP and ADAP-YFP were seeded and were fixed 3 min after the initiation of the spreading process. The average value of FRET efficiency ± standard error obtained for a given pair is shown. The data shown are representative of >3 independent experiments.

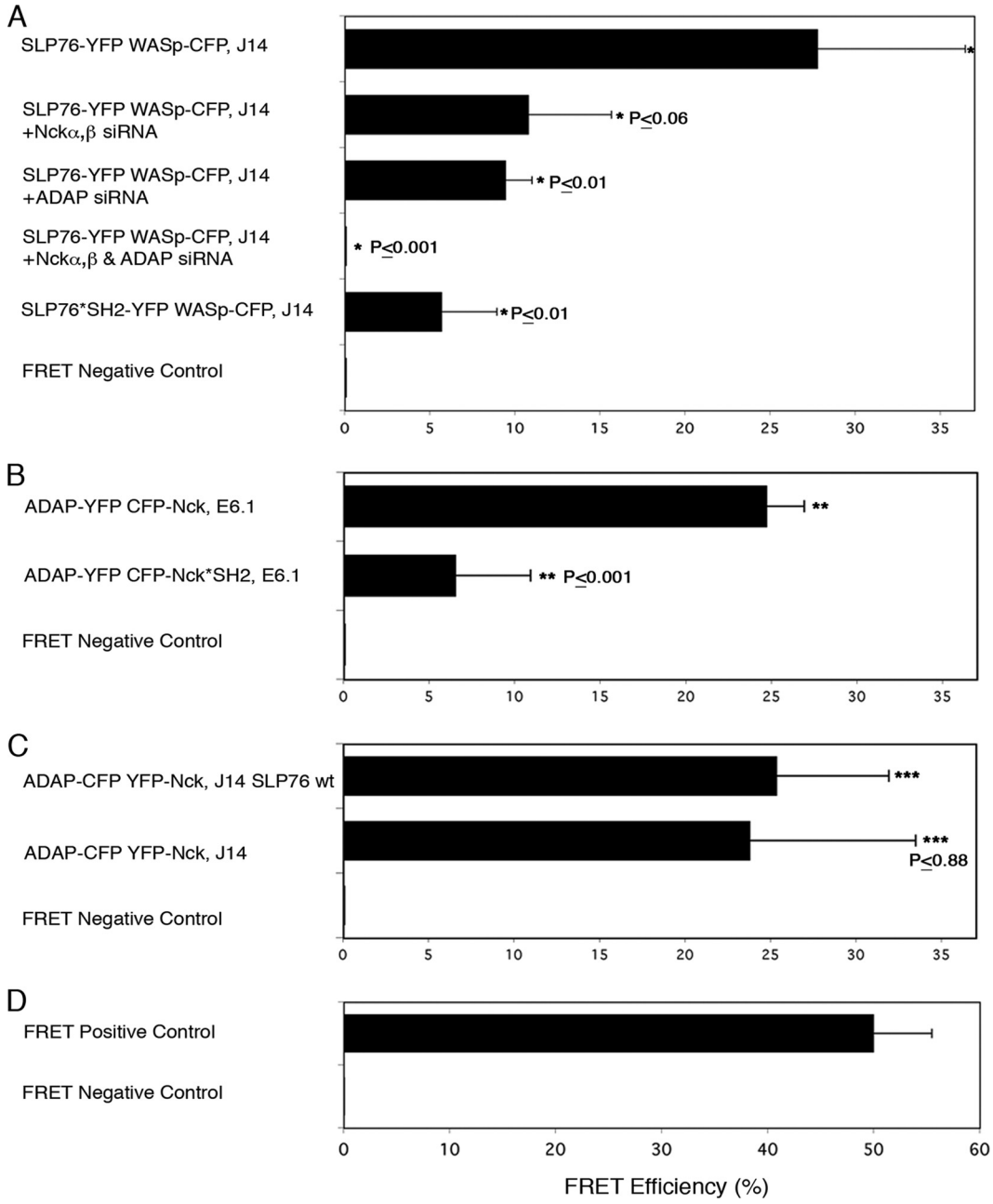

FIG. 5. Both Nck and ADAP participate in stabilizing the SLP76 interaction with WASp. (A) J14 cells, expressing SLP76-YFP and WASp-CFP and pretreated with specific siRNA, were seeded and fixed. The colocalization between SLP76 and WASp was observed and calculated for >3 independent experiments. FRET analysis is shown. *t* tests were performed comparing the results of NS siRNA treatment to the results of specific siRNA treatment for other experimental groups. (B, C) FRET analysis of the molecular associations between ADAP and Nck. Various cell types were seeded and were fixed 3 min into the spreading process. The average value of FRET efficiency ± standard error obtained for a given pair is shown. The data are representative of >3 independent experiments. (D) Results for FRET positive controls (cells expressing CFP and YFP encoded on the same plasmid, i.e., maximal FRET obtained in this system) and negative controls (CFP and YFP expressed by different plasmids and undergoing minimal FRET, i.e., only that produced by random colocalizations).

SLP76 SH2 domain (10.5% ± 1.45%; $P \leq 0.0002$) (Fig. 3A, bottom, and B). This result indicates that partial association between SLP76 and ADAP occurs independently of the SLP76 SH2 domain. This result is in agreement with the immunoprecipitation data (see Fig. S5B in the supplemental material) and suggests alternative ways for recruiting ADAP to SLP76, potentially by the Nck-WASp complex.

Next, we analyzed the interaction between Nck and ADAP. The results of recent studies suggested that Nck associates directly with ADAP (28, 29). In order to examine this interaction *in vivo* in our system, we used FRET analysis to investigate the binding of ADAP to the Nck SH2 domain. E6.1 Jurkat T cells expressing ADAP-YFP and CFP-Nck wt versus the CFP-Nck SH2 mutant (K308W, CFP-Nck*SH2) were analyzed for

FRET efficiency. The FRET data clearly demonstrate that these proteins interact (24.7% ± 2.2%), and the mutation at the Nck SH2 domain dramatically decreased FRET efficiency (6.55% ± 4.4%) (Fig. 5B, $P < 0.001$). Interestingly, the FRET was not reduced to zero, most probably due to a weak indirect interaction between Nck and ADAP via WASp. In addition, we checked the interactions between Nck and ADAP in the presence and absence of SLP76. SLP76-deficient J14 cells expressing ADAP-YFP and CFP-Nck were compared to J14 cells reconstituted with SLP76 wt, and the FRET efficiency was measured in both experimental systems. Our data indicate no significant difference in this protein interaction in the presence (25.4% ± 6.5%) or absence (23.8% ± 9.7%) of SLP76 ($P \leq 0.88$) (Fig. 5C).

Since intramolecular associations between signaling proteins in a complex are difficult to follow by a biochemical approach, we decided to study the Nck requirement for a putative SLP76-Nck-WASp-ADAP tetramolecular interaction by FRET analysis. SLP76*SH2-YFP- and ADAP-CFP-expressing J14 cells were transiently transfected with siRNA specific for Nckα,β. Inhibition of Nckα,β expression dramatically reduced the FRET between SLP76 and ADAP ($P \leq 0.00004$) (Fig. 3B), suggesting a cooperatively assembled tetramolecular signaling complex composed of SLP76, ADAP, Nck, and WASp following T cell activation. The results for FRET negative and positive controls are shown in Fig. 5D.

Nck and ADAP contribute to actin rearrangement in a complementary fashion. We then examined the requirement of the SLP76-Nck-WASp-ADAP tetramolecular interaction for actin rearrangement. First, we tested the role of Nck and ADAP interactions for this activity. ADAP-deficient T cells (JDAP) were gene silenced for endogenous Nck by using siRNA specific to the SH2 domain of Nck (see Fig. S2C in the supplemental material for siRNA efficiency), and their actin rearrangement was compared to that in cells expressing the YFP-NckΔSH2 mutant (see Fig. S7A in the supplemental material). No differences in actin rearrangement were observed ($P \leq 0.38$). The actin shape index was completely impaired (2.25 ± 0.09 versus 2.14 ± 0.08, respectively), suggesting the requirement of the Nck SH2 domain in mediating the interactions between WASp and both SLP76 and ADAP, as expected.

Next, in order to check the role of Nck and/or ADAP in this system, we used J14 cells expressing SLP76-YFP and WASp-CFP. The application of siRNA specific for Nckα,β or ADAP resulted in the partial impairment of actin distribution (Fig. 6); however, treating the cells with siRNA to both Nckα,β and ADAP dramatically abolished actin rearrangement, as measured by the actin shape index (Fig. 6, bottom image and graph). Both the spreading of the cells and actin rearrangement were poor, suggesting the requirement of both Nck and ADAP for optimal actin rearrangement.

Furthermore, in order to study the role of SLP76-ADAP interactions in actin rearrangement, ADAP-deficient T cells transfected with ADAP wt or ADAP mutated in SLP76 binding sites Y595, 651F were used, and their actin shape indices were compared. Our results demonstrate that the interaction of ADAP with SLP76 is important not only for SLP76-WASp interactions (Fig. 5A) but also for actin rearrangement, as shown in Fig. S7B in the supplemental material. Actin rearrangement of ADAP-deficient T cells expressing ADAP wt versus ADAP Y595, 651F was dramatically impaired, as indicated by an increase in the actin shape index, the indices being 1.38 ± 0.03 versus 2.69 ± 0.11, respectively ($P < 0.00003$).

To confirm that the results obtained in transformed cell lines apply to primary T cells, human peripheral blood lymphocytes (PBLs) were isolated and transiently transfected with siRNA to Nckα,β or ADAP (Fig. 7A). Effects similar to those observed in Jurkat cells were detected in PBLs (Fig. 7B). Inhibition of Nckα,β or ADAP expression caused a slight impairment in actin rearrangement. However, inhibition of all three not only caused severe damage in actin distribution ($P \leq 0.000005$) but also severely altered cell shape and spreading. Taken together, these data suggest that Nckα,β and ADAP participate cooperatively to stabilize the interaction between SLP76 and WASp and to transduce the signal to actin polymerization (see Fig. S8 in the supplemental material).

DISCUSSION

The activation of human T cells via stimulation of the TCR is critical for the immune response to pathogens. The signaling cascades linking the TCR to actin polymerization play a critical role in controlling vital cellular properties, such as cell shape, motility, and proliferation. Many molecules involved in TCR-mediated actin polymerization have been described, including SLP76, Nck, WASp (4, 8, 26), WAVE2 (33, 34), HS1, and formins (20, 21, 39). The results of a previous study suggest that the Nck carboxyl-terminal SH3 domain is critical for the recruitment of WASp to the IS (51); however, these data are based on the transient overexpression of a Nck mutant in the presence of endogenous Nck. In our current study, we demonstrated for the first time that Nck is not uniquely required for SLP76-WASp interactions. Using a gene-silencing approach, we examined the roles of the two Nck isoforms in actin rearrangement and the recruitment of WASp to SLP76 signaling complexes. We showed that although Nckα and β had overlapping functions, together they were not sufficient for optimal recruitment of WASp to the SLP76 complex. We defined a new role for the adapter molecule ADAP in WASp recruitment and demonstrated novel cooperative molecular interactions between SLP76, Nck, ADAP, and WASp in the TCR-mediated actin machinery. T cells stably expressing an SLP76 mutant in which tyrosines 112, 128, and 145 are mutated to phenylalanine fail to efficiently recruit Nck to the T-B cell contact site (51). This suggests that the interaction of Nck with tyrosine-phosphorylated SLP76 is mediated by the Nck SH2 domain. In agreement with these results, we showed that a deletion or mutation of the SH2 domain caused a slightly dispersed pattern of Nck upon TCR induction. However, the SLP76-Nck association did not depend solely on the Nck SH2 domain, since a partial colocalization between SLP76 and Nck SH2 domain mutants was still observed. Furthermore, recruitment of WASp to SLP76 signaling clusters was detected in the setting of Nck suppression, suggesting an alternative pathway linking the SLP76 signaling complex to WASp and the actin polymerization machinery.

SLP76 is known to bind the ADAP adapter molecule via its SH2 domain upon phosphorylation of ADAP tyrosine residue 651 (15, 19, 32). Indeed, using FRET analysis, we demonstrated that a point mutation, Y651F, in ADAP caused a dra-

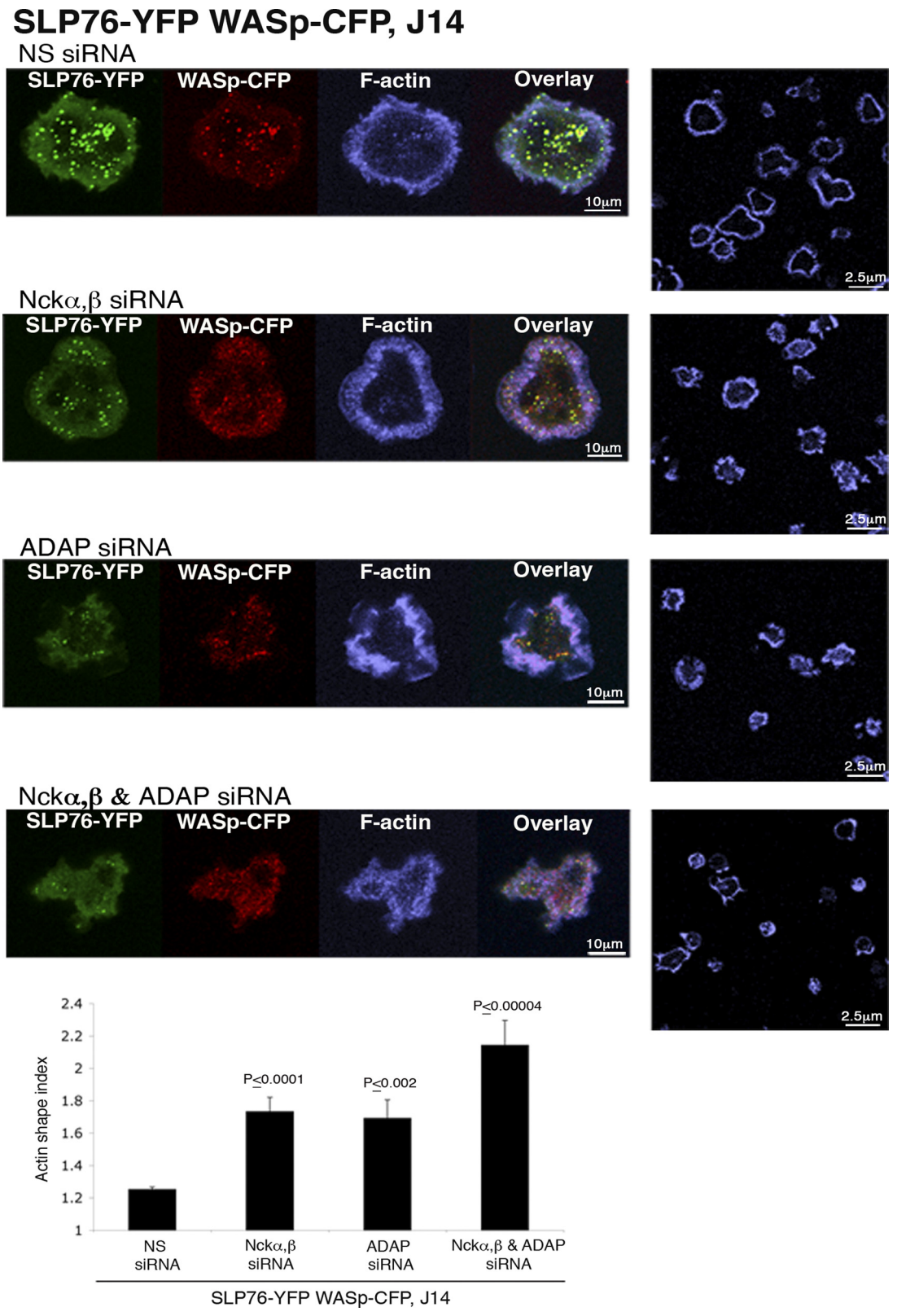

FIG. 6. Nck and ADAP are both required for actin rearrangement. SLP76-deficient J14T cells expressing SLP76-YFP and WASp-CFP were pretreated with siRNA specific for Nckα,β and/or ADAP and were plated for 5 min on stimulatory coverslips, fixed, and stained with phalloidin (blue). Confocal images were obtained at the coverslip. The fluorescence images of SLP76-YFP, WASp-CFP, and phalloidin staining are shown. Representative fields of cells stained with phalloidin are shown for conditions in the panels on the right. The final panel shows a graph of the actin shape index obtained from the phalloidin-stained images of each sample, as explained in Materials and Methods. A graph of the results of 4 independent experiments is presented; error bars show standard errors. The results of *t* tests between cells treated with NS siRNA and each experimental group are presented. Significant differences were found between cells treated with Nck or ADAP siRNA and cells treated with both Nck and ADAP siRNA, with *P* values of ≤0.029 and ≤0.026, respectively.

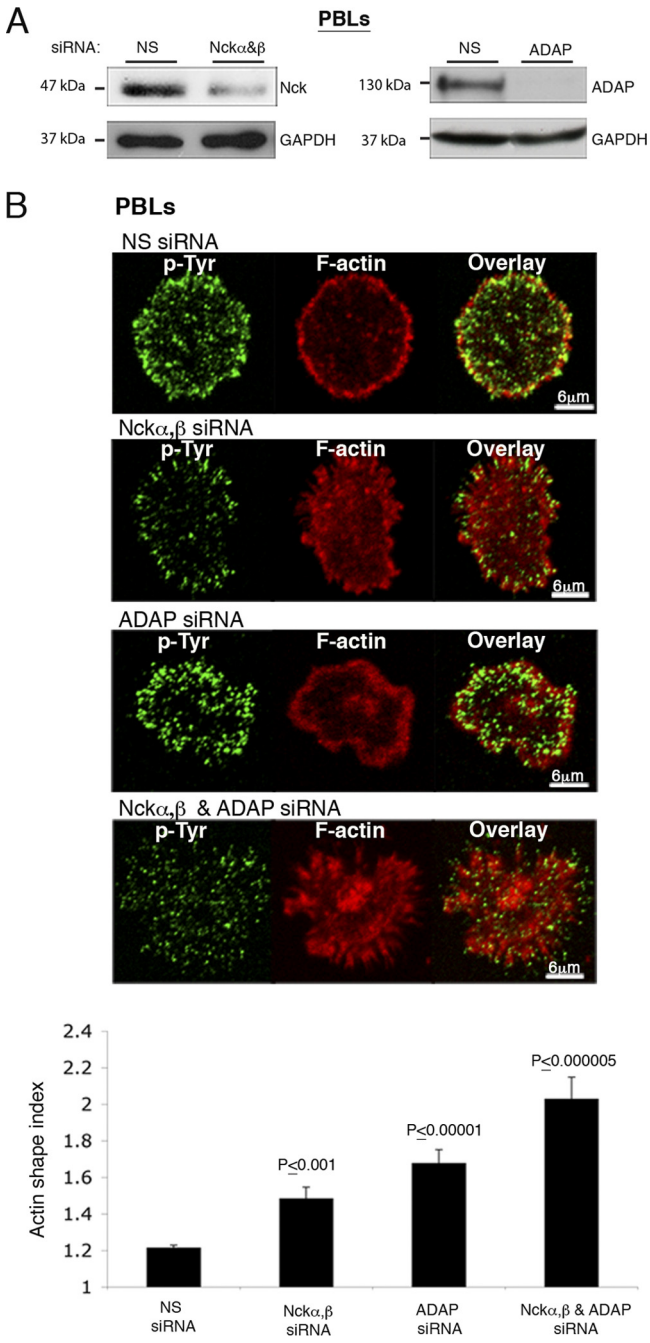

FIG. 7. Nck and ADAP are both required for actin rearrangement, as was detected in PBLs. (A) PBLs were treated with siRNA specific to Nckα,β or ADAP. After 48 h, cell lysates were prepared and analyzed for protein levels. The siRNA-mediated ADAP or Nck downregulation was compared to the level of GAPDH (glyceraldehyde-3-phosphate dehydrogenase). (B) Nckα,β and ADAP knockdown experiments of were performed with human PBLs. PBLs pretreated with siRNA specific for Nckα,β and/or ADAP were seeded on stimulatory coverslips coated with anti-CD3 and anti-CD28. After 20 min of spreading, cells were fixed and stained with phalloidin (red). Overlay images and a summary of the results of 3 independent experiments (bottom) are presented. The actin spreading index was determined as described in Materials and Methods. *t* tests were calculated between cells treated with NS siRNA and the experimental groups. Gene silencing of both Nckα,β and ADAP caused a dramatic impairment of actin rearrangement in comparison to that in cells treated with NS siRNA ($P < 0.000005$). Slight impairments were detected in cells treated with Nckα,β or ADAP siRNA ($P < 0.001$ and $P < 0.00001$, respectively). *t* test analyses between the results for Nck or ADAP siRNA and a combined treatment with both Nck and ADAP siRNA were performed, and the *P* values were <0.00061 and 0.02, respectively.

matic reduction in the FRET efficiency between SLP76 and ADAP. In functional studies, we showed that RNA interference-mediated silencing of ADAP caused effects similar to the SLP76 SH2 domain mutation, including a decreased retention of SLP76 molecules at the TCR and a slight impairment of actin polymerization. The role of ADAP in integrin-mediated adhesion controlled by TCR-induced inside-out signaling is well known (36, 45, 46); however, the involvement of ADAP in the actin cytoskeleton is a matter of debate (35). Previously, it was shown that ADAP-deficient T cells do not present any impairment in actin polymerization (22). However, confocal studies revealed that ADAP colocalizes with F-actin filaments (18), and ADAP was recently shown to be involved in outside-in and inside-out T cell signaling, which are known to involve the actin machinery (43, 46).

Our studies point to a novel role of ADAP in TCR-mediated events and the actin machinery. Suppression of both ADAP and the two Nck isoforms completely blocked the interaction between SLP76 and WASp, as quantified by FRET analysis, and caused a severe defect in actin reorganization. These data strongly suggest that ADAP mediates an interaction between SLP76 and WASp. In addition, biochemical and FRET analyses indicated that ADAP constitutively interacted with WASp independent of TCR activation or SLP76. Furthermore, the SLP76-WASp interaction did not depend exclusively either on Nck isoforms or on ADAP. WASp was still recruited to SLP76 signaling complexes in the absence of Nckα,β or in the presence of SLP76*SH2. Thus, we concluded that optimal actin polymerization, mediated by the TCR through SLP76, involves both Nck and ADAP interactions with WASp, and we suggest that a tetramolecular complex of SLP76, Nck, ADAP, and WASp is formed by TCR activation.

Multiple results confirm the interaction of these four molecules and the presence of a tetramolecular complex at the site of TCR engagement. We demonstrated that the recruitment of ADAP to SLP76 did not solely depend on the SLP76 SH2 domain, since positive FRET was detected between the two molecules in SLP76-deficient T cells exclusively expressing the SH2 mutant form of SLP76. Gene silencing of both Nck isoforms in these cells caused a dramatic reduction in the FRET efficiency between SLP76 and ADAP, suggesting that the Nck-WASp interaction served as an alternative pathway for recruiting ADAP in the absence of a functional SLP76 SH2 domain. The results of our study emphasize that the elimination of a single link in this tetramolecular complex dramatically reduces the functional activity of each component and adversely affects actin reorganization (as demonstrated in Fig. S8 in the supplemental material). Recently, Lettau et al. demonstrated by a two-hybrid system an association between Nck and ADAP (28). This finding supports our data on the existence of a tetrameric complex consisting of SLP76, Nck, ADAP, and WASp following TCR stimulation.

Regulation of actin polymerization in mammalian T cells involves other WASp-related proteins, including WAVE2 (33). These proteins are highly conserved, especially at the carboxyl-terminal VCA domain, which is responsible for the interaction with monomeric and filamentous actin, as well as the Arp2/3 complex (3). We demonstrated that the impairment in actin polymerization observed in cells lacking Nck and ADAP proteins correlated with a lack of WASp recruitment to SLP76 signaling complexes. However, although the WASp family proteins share a redundant role in lamelliopodium formation and actin polymerization, it will be valuable in the future to check the role of Nck and ADAP in alternative actin polymerization pathways involving other members of the WASp family, e.g., WAVE2.

ACKNOWLEDGMENTS

We thank Lawrence E. Samelson for his helpful advice and discussions, Alex Braiman and Jon C. D. Houtman for technical assistance, and Valarie Barr and Nathan Coussens for critical reading of the manuscript.

This research was funded by the Israeli Ministry of Health through the Office of the Chief Scientist and by the Israel Science Foundation (grants 1659/08 and 971/08).

REFERENCES

1. **Badour, K., et al.** 2004. Fyn and PTP-PEST-mediated regulation of Wiskott-Aldrich syndrome protein (WASp) tyrosine phosphorylation is required for coupling T cell antigen receptor engagement to WASp effector function and T cell activation. J. Exp. Med. **199:**99–112.
2. **Badour, K., et al.** 2003. The Wiskott-Aldrich syndrome protein acts downstream of CD2 and the CD2AP and PSTPIP1 adaptors to promote formation of the immunological synapse. Immunity **18:**141–154.
3. **Badour, K., J. Zhang, and K. A. Siminovitch.** 2004. Involvement of the Wiskott-Aldrich syndrome protein and other actin regulatory adaptors in T cell activation. Semin. Immunol. **16:**395–407.
4. **Barda-Saad, M., et al.** 2005. Dynamic molecular interactions linking the T cell antigen receptor to the actin cytoskeleton. Nat. Immunol. **6:**80–89.
5. **Barda-Saad, M., et al.** 2010. Cooperative interactions at the SLP-76 complex are critical for actin polymerization. EMBO J. **29:**2315–2328.
6. **Barr, V. A., et al.** 2006. T-cell antigen receptor-induced signaling complexes: internalization via a cholesterol-dependent endocytic pathway. Traffic **7:**1143–1162.
7. **Braiman, A., M. Barda-Saad, C. L. Sommers, and L. E. Samelson.** 2006. Recruitment and activation of PLCgamma1 in T cells: a new insight into old domains. EMBO J. **25:**774–784.
8. **Bubeck Wardenburg, J., et al.** 1998. Regulation of PAK activation and the T cell cytoskeleton by the linker protein SLP-76. Immunity **9:**607–616.
9. **Bunnell, S. C., et al.** 2002. T cell receptor ligation induces the formation of dynamically regulated signaling assemblies. J. Cell Biol. **158:**1263–1275.
10. **Burbach, B. J., R. B. Medeiros, K. L. Mueller, and Y. Shimizu.** 2007. T-cell receptor signaling to integrins. Immunol. Rev. **218:**65–81.
11. **Cannon, J. L., et al.** 2001. Wasp recruitment to the T cell:APC contact site occurs independently of Cdc42 activation. Immunity **15:**249–259.
12. **Charrin, S., and A. Alcover.** 2006. Role of ERM (ezrin-radixin-moesin) proteins in T lymphocyte polarization, immune synapse formation and in T cell receptor-mediated signaling. Front. Biosci. **11:**1987–1997.
13. **Cory, G. O., R. Garg, R. Cramer, and A. J. Ridley.** 2002. Phosphorylation of tyrosine 291 enhances the ability of WASp to stimulate actin polymerization and filopodium formation. Wiskott-Aldrich syndrome protein. J. Biol. Chem. **277:**45115–45121.
14. **Custodio, N., M. Vivo, M. Antoniou, and M. Carmo-Fonseca.** 2007. Splicing- and cleavage-independent requirement of RNA polymerase II CTD for mRNA release from the transcription site. J. Cell Biol. **179:**199–207.
15. **da Silva, A. J., et al.** 1997. Cloning of a novel T-cell protein FYB that binds FYN and SH2-domain-containing leukocyte protein 76 and modulates interleukin 2 production. Proc. Natl. Acad. Sci. U. S. A. **94:**7493–7498.
16. **Dombroski, D., et al.** 2005. Kinase-independent functions for Itk in TCR-induced regulation of Vav and the actin cytoskeleton. J. Immunol. **174:**1385–1392.
17. **Donnadieu, E., M. H. Jouvin, and J. P. Kinet.** 2000. A second amplifier function for the allergy-associated Fc(epsilon)RI-beta subunit. Immunity **12:**515–523.
18. **Geng, L., S. Pfister, S. K. Kraeft, and C. E. Rudd.** 2001. Adaptor FYB (Fyn-binding protein) regulates integrin-mediated adhesion and mediator release: differential involvement of the FYB SH3 domain. Proc. Natl. Acad. Sci. U. S. A. **98:**11527–11532.
19. **Geng, L., M. Raab, and C. E. Rudd.** 1999. Cutting edge: SLP-76 cooperativity with FYB/FYN-T in the up-regulation of TCR-driven IL-2 transcription requires SLP-76 binding to FYB at Tyr595 and Tyr651. J. Immunol. **163:** 5753–5757.
20. **Gomez, T. S., et al.** 2007. Formins regulate the actin-related protein 2/3 complex-independent polarization of the centrosome to the immunological synapse. Immunity **26:**177–190.
21. **Gomez, T. S., et al.** 2006. HS1 functions as an essential actin-regulatory adaptor protein at the immune synapse. Immunity **24:**741–752.
22. **Griffiths, E. K., et al.** 2001. Positive regulation of T cell activation and integrin adhesion by the adapter Fyb/Slap. Science **293:**2260–2263.
23. **Griffiths, E. K., and J. M. Penninger.** 2002. Communication between the TCR and integrins: role of the molecular adapter ADAP/Fyb/Slap. Curr. Opin. Immunol. **14:**317–322.
24. **Huang, Y., et al.** 2005. Deficiency of ADAP/Fyb/SLAP-130 destabilizes SKAP55 in Jurkat T cells. J. Biol. Chem. **280:**23576–23583.
25. **Jordan, M. S., A. L. Singer, and G. A. Koretzky.** 2003. Adaptors as central mediators of signal transduction in immune cells. Nat. Immunol. **4:**110–116.
26. **Krause, M., et al.** 2000. Fyn-binding protein (Fyb)/SLP-76-associated protein (SLAP), Ena/vasodilator-stimulated phosphoprotein (VASP) proteins and the Arp2/3 complex link T cell receptor (TCR) signaling to the actin cytoskeleton. J. Cell Biol. **149:**181–194.
27. **Laurence, A., E. Astoul, S. Hanrahan, N. Totty, and D. Cantrell.** 2004. Identification of pro-interleukin 16 as a novel target of MAP kinases in activated T lymphocytes. Eur. J. Immunol. **34:**587–597.
28. **Lettau, M., et al.** 2010. The adapter protein Nck: role of individual SH3 and SH2 binding modules for protein interactions in T lymphocytes. Protein Sci. **19:**658–669.
29. **Lettau, M., J. Pieper, and O. Janssen.** 2009. Nck adapter proteins: functional versatility in T cells. Cell Commun. Signal. **7:**1.
30. **Mabon, S. A., and T. Misteli.** 2005. Differential recruitment of pre-mRNA splicing factors to alternatively spliced transcripts in vivo. PLoS Biol. **3:**e374.
31. **Miyoshi-Akiyama, T., L. M. Aleman, J. M. Smith, C. E. Adler, and B. J. Mayer.** 2001. Regulation of Cbl phosphorylation by the Abl tyrosine kinase and the Nck SH2/SH3 adaptor. Oncogene **20:**4058–4069.
32. **Musci, M. A., et al.** 1997. Molecular cloning of SLAP-130, an SLP-76-associated substrate of the T cell antigen receptor-stimulated protein tyrosine kinases. J. Biol. Chem. **272:**11674–11677.
33. **Nolz, J. C., et al.** 2006. The WAVE2 complex regulates actin cytoskeletal reorganization and CRAC-mediated calcium entry during T cell activation. Curr. Biol. **16:**24–34.
34. **Nolz, J. C., et al.** 2007. WAVE2 regulates high-affinity integrin binding by recruiting vinculin and talin to the immunological synapse. Mol. Cell. Biol. **27:**5986–6000.
35. **Peterson, E. J.** 2003. The TCR ADAPts to integrin-mediated cell adhesion. Immunol. Rev. **192:**113–121.
36. **Peterson, E. J., et al.** 2001. Coupling of the TCR to integrin activation by Slap-130/Fyb. Science **293:**2263–2265.
37. **Samelson, L. E.** 2002. Signal transduction mediated by the T cell antigen receptor: the role of adapter proteins. Annu. Rev. Immunol. **20:**371–394.
38. **Sauer, K., et al.** 2001. Hematopoietic progenitor kinase 1 associates physically and functionally with the adaptor proteins B cell linker protein and SLP-76 in lymphocytes. J. Biol. Chem. **276:**45207–45216.
39. **Schwartzberg, P. L.** 2007. Formin the way. Immunity **26:**139–141.
40. **Sechi, A. S., J. Buer, J. Wehland, and M. Probst-Kepper.** 2002. Changes in actin dynamics at the T-cell/APC interface: implications for T-cell anergy? Immunol. Rev. **189:**98–110.
41. **Shen, S., et al.** 2009. The importance of Src homology 2 domain-containing leukocyte phosphoprotein of 76 kilodaltons sterile-alpha motif domain in thymic selection and T-cell activation. Blood **114:**74–84.
42. **Singh, S., M. Plassmeyer, D. Gaur, and L. H. Miller.** 2007. Mononeme: a new secretory organelle in Plasmodium falciparum merozoites identified by localization of rhomboid-1 protease. Proc. Natl. Acad. Sci. U. S. A. **104:** 20043–20048.
43. **Suzuki, J., S. Yamasaki, J. Wu, G. A. Koretzky, and T. Saito.** 2007. The actin cloud induced by LFA-1-mediated outside-in signals lowers the threshold for T-cell activation. Blood **109:**168–175.
44. **Torres, E., and M. K. Rosen.** 2006. Protein-tyrosine kinase and GTPase signals cooperate to phosphorylate and activate Wiskott-Aldrich syndrome protein (WASP)/neuronal WASP. J. Biol. Chem. **281:**3513–3520.
45. **Wang, H., et al.** 2004. ADAP-SLP-76 binding differentially regulates supramolecular activation cluster (SMAC) formation relative to T cell-APC conjugation. J. Exp. Med. **200:**1063–1074.
46. **Wang, H., B. Wei, G. Bismuth, and C. E. Rudd.** 2009. SLP-76-ADAP adaptor module regulates LFA-1 mediated costimulation and T cell motility. Proc. Natl. Acad. Sci. U. S. A. **106:**12436–12441.
47. **Weiss, A.** 2010. The right team at the right time to go for a home run: tyrosine kinase activation by the TCR. Nat. Immunol. **11:**101–104.
48. **Wu, J. N., and G. A. Koretzky.** 2004. The SLP-76 family of adapter proteins. Semin. Immunol. **16:**379–393.
49. **Wunderlich, L., A. Farago, J. Downward, and L. Buday.** 1999. Association of

Nck with tyrosine-phosphorylated SLP-76 in activated T lymphocytes. Eur. J. Immunol. **29:**1068–1075.
50. **Zacharias, D. A., J. D. Violin, A. C. Newton, and R. Y. Tsien.** 2002. Partitioning of lipid-modified monomeric GFPs into membrane microdomains of live cells. Science **296:**913–916.
51. **Zeng, R., et al.** 2003. SLP-76 coordinates Nck-dependent Wiskott-Aldrich syndrome protein recruitment with Vav-1/Cdc42-dependent Wiskott-Aldrich syndrome protein activation at the T cell-APC contact site J. Immunol. **171:**1360–1368.
52. **Zipfel, P. A., et al.** 2006. Role for the Abi/wave protein complex in T cell receptor-mediated proliferation and cytoskeletal remodeling. Curr. Biol. **16:**35–46.